



<https://doi.org/10.1590/2318-0331.252020190070>

Combination of experimental and numerical approaches to determine the main characteristics of skimming flow in stepped spillways

Combinação de abordagens experimental e numérica para determinar as principais características do escoamento sobre turbilhões em vertedouros em degraus

Lucas Camargo da Silva Tassinari¹ , Daniela Guzzon Sanagiotto¹ , Marcelo Giulian Marques¹ ,
Luísa Lüdtke Lauffer¹  & Edgar Fernando Trierweiler Neto² 

¹Instituto de Pesquisas Hidráulicas, Universidade Federal do Rio Grande do Sul, Porto Alegre, RS, Brasil

²Eletrobras Furnas, Rio de Janeiro, RJ, Brasil

E-mails: lucascstassinari@gmail.com (LCST), dsanagiotto@ufrgs.br (DGS), mmarques@iph.ufrgs.br (MGM), luisalauffer@gmail.com (LLL), edtrier@furnas.com.br (EFTN)

Received: May 29, 2019 - Revised: September 23, 2019 - Accepted: October 15, 2019

ABSTRACT

The traditional approach for the hydrodynamic characterization of the flow down stepped spillways is through physical modeling, which is susceptible to scale effects and has limitations related to experimental apparatus, laboratory space and the spatial discretization of data collection. Computational fluid dynamics (CFD) is an important tool for hydrodynamic analysis because, if used properly, it presents great potential for application in hydraulics. In this work, CFD was used to model the skimming flow down a stepped spillway to investigate the effects of possible pressure measurement errors due to uncertainties in the position of the sensors within the steps. The numerical model was validated through literature velocity profiles and pressure experimental data. The results showed that the best values of water fraction (α) to define free surface are $\alpha = 0.30$ in the nonaerated region and $\alpha = 0.10$ in the aerated region. Statistical parameters were calculated using experimental data to estimate extreme pressures. These parameters and the simulation results were used to determine that the extreme maximum and minimum pressures occur, respectively, in the region of $0.81 < x/l < 0.98$, in the horizontal faces, and in the region of $0.93 < y/h < 0.98$, in the vertical faces.

Keywords: Stepped spillways; CFD; Free surface; Turbulence; Pressure.

RESUMO

A abordagem tradicional para a caracterização hidrodinâmica do escoamento sobre vertedouros em degraus é feita através da modelagem física, a qual é suscetível aos efeitos de escala e possui limitações relacionadas ao aparato experimental, espaço físico de laboratório e discretização espacial da obtenção de dados. A fluidodinâmica computacional é uma importante ferramenta de análise dos escoamentos, pois, se utilizada corretamente, apresenta grande potencial de aplicação na engenharia hidráulica. Neste trabalho, foi utilizada fluidodinâmica computacional para modelar o escoamento deslizando sobre turbilhões em um vertedouro em degraus. Buscou-se investigar os efeitos de possíveis erros de medição de pressão devido às incertezas na posição dos medidores dentro dos degraus. O modelo numérico foi validado através de dados de pressão obtidos experimentalmente e dados de velocidade encontrados na literatura. Os resultados mostram que os melhores valores de fração de água (α) que definem a superfície livre são $\alpha = 0,30$ para a região não aerada e $\alpha = 0,10$ para a região aerada. Utilizando-se dados experimentais, foram calculados parâmetros estatísticos para estimar pressões extremas. O uso destes parâmetros, em conjunto com os resultados das simulações, permite definir que as pressões extremas positivas ocorrem na região $0,81 < x/l < 0,98$ nos patamares e as mínimas na região $0,93 < y/h < 0,98$ nos espelhos.

Palavras-chave: Vertedouro em degraus; CFD; Superfície livre; Turbulência; Pressão.



INTRODUCTION

When spillways are constructed in steps, part of the energy of the flow dissipates along the spillway itself, allowing to reduce the dimensions of the energy dissipation structures constructed downstream of the dams (Chen et al., 2002; Frizell & Frizell, 2015; Sanagiotta & Marques, 2008; Simões et al., 2010; Tabari & Tavakoli, 2016), generating significant financial savings.

There are two approaches to estimate the characteristics of air-water two-phase flows down stepped structures: physical modeling and numerical simulation, and both approaches have uncertainties (Pfister & Hager, 2014). Physical modeling is susceptible to scale effects and has limitations related to the spatial discretization of data collection, instrumentation and available laboratory infrastructure (e.g., physical space and pumping capacity). Computational numerical modeling, therefore, emerges as an important tool for analyzing flows, providing greater flexibility to study hydraulic structures with different configurations. However, the quality of the results is sensitive to the turbulence model, the grid quality, the calibration and the validation of the results, among others.

Traditionally, the approach of hydrodynamic characterization of flow down stepped spillways is done through physical modeling (Amador et al., 2009; Chanson, 1993; Gomes, 2006; Sanagiotta & Marques, 2008; Tozzi, 1992; Zhang & Chanson, 2016a, 2016b), from which it was possible to characterize the flow on different configurations of stepped spillways by analyzing average and instantaneous pressures, energy dissipation and aeration in structures with chutes of different slopes, such as: 1.0V:0.75H (e.g., Meireles et al., 2012; Sanagiotta & Marques, 2008), 1.0V:0.8H (e.g., Amador et al., 2009; Sánchez-Juny et al., 2007), 1.0V:1.0H (e.g., Dai Prá et al., 2012; Simões et al., 2013; Zhang & Chanson, 2016a), 1.0V:2.0H (e.g., Bung, 2011), among others.

From these works, it is concluded that, in general, the negative pressures appear on the vertical faces of the steps, with its upper end being the region where the negative pressures with largest magnitudes are expected (Amador et al., 2009; Chen et al., 2002; Lobosco & Schulz, 2010; Zhang et al., 2012). The most important positive pressures appear on the horizontal face, in the region near the external edge of the step (Dai Prá et al., 2012; Sanagiotta, 2003), or in relative positions between 75 and 80% of the total horizontal face length, as verified by Zhang et al. (2012).

Zhang et al. (2012) studied pressures along the chute in the nonaerated and gradually aerated regions of the flow down a 1.0V:2.0H stepped spillway model. At the horizontal faces, the authors observed a variation of the pressures in the form of an “S”, so that the most extreme pressures are not exactly at the ends of horizontal faces, but at some distance from these points. In the vertical faces, negative pressures occur in a region very close to the outer step edge, and become more extreme as the flow rates increase.

Gomes (2006) studied the pressure coefficients along the steps as a function of the dimensionless longitudinal position S' , which is defined as:

$$S' = \frac{L - La}{ha} \quad (1)$$

where: L = longitudinal distance measured along the chute parallel to the pseudobottom; La = length until the inception point, both measured from the beginning of the crest of the spillway; and ha = depth in the inception point.

The root mean square pressure coefficient, defined by Equation 2, presented smooth growth for $S' \leq -7$, with a peak around $S' \approx 0$. At $S' \approx 4$, the process of attenuation of extreme pressures and pressure fluctuations initiate. As a consequence, the pressure coefficients values were more critical in the range of $0 \leq S' \leq 4$.

$$C_{\sigma_p} = \frac{\sigma_p}{\frac{u_m^2}{2 \cdot g}} \quad (2)$$

where: C_{σ_p} = root mean square pressure coefficient; σ_p = root mean square of pressure fluctuations; u_m = mean flow velocity; and g = gravitational acceleration.

The flows found in engineering practice are predominantly turbulent and therefore require special treatment (Ferziger & Peric, 2002). Turbulent flows are highly unsteady and composed of three-dimensional vortices with different sizes and quantities of energy whose details can be studied with the aid of physical experiments or numerical solutions of the flow-governing equations (Ferziger & Peric, 2002; Simões, 2012). The governing equations (conservation of mass, momentum and energy) are discretized and solved numerically for the domain of interest using computational fluid dynamics (CFD) tools.

In turbulent flows, the fluctuations of transport of mass, momentum and energy can be of small scale and high frequency, and may incur a high computational cost when simulated with direct numerical simulations (DNS).

Thus, instead of using the equations for instantaneous quantities, time-averaged values or manipulations can be used to remove small scales. However, as a result, additional unknown variables emerge, which require turbulence models to solve the governing equations and enable their closure. This is what is done in the Reynolds-Averaged Navier-Stokes (RANS) numerical simulation technique, in which all the unsteadiness are separated into mean values and fluctuations, which are modeled with turbulence models (Arantes, 2007; Ferziger & Peric, 2002).

The correct selection of the turbulence model is important to simulate the boundary layer development properly (Lopes et al., 2018; Qian et al., 2009). However, some works developed specifically for stepped spillways have shown that the choice of turbulence model has little influence on velocity profiles above the pseudobottom (Bombardelli et al., 2011; Kositgittiwong et al., 2013; Qian et al., 2009), water depths (Bombardelli et al., 2011; Daneshfaraz et al., 2016) and pressure fields (Bai & Zhang, 2017).

To our knowledge, Chen et al. (2002) were the first researchers to simulate flow down a stepped spillway with a numerical turbulence model. These authors used a numerical model with an unstructured mesh, the Volume of Fluid (VOF) method (Hirt & Nichols, 1981) to treat the free surface and the $k-\epsilon$ model (Jones & Launder, 1972; Launder & Spalding, 1974) for the turbulence closure.

Since then, several other studies have used numerical simulation to evaluate flows along stepped spillways. Bombardelli et al. (2011)

compared experimental and numerical results of discharge, depth values and velocity profiles in a stepped spillway with a focus on the nonaerated region, important for the flow down spillways in small dams or with large specific discharges. The simulations were performed with FLOW-3D software, with structured meshes, with free surface treatment with the TruVOF model and the turbulence models $k-\epsilon$ and RNG $k-\epsilon$. In analyzing the results of the simulations with the different models of turbulence, the authors verified that the $k-\epsilon$ model offers good results in terms of depths and velocities, with differences of 1% for velocities and 0.5% for the discharges between the different models of turbulence.

Later, Meireles et al. (2014) analyzed the position of the inception point in skimming flow down stepped spillways, comparing experimental data (Bombardelli et al., 2011) and numerical data obtained with FLOW-3D software, using five different methodologies to establish this position.

The experimental methodologies consisted of: (i) observing where the boundary layer intercepts the free surface and (ii) observing where the white coloration in the water appeared due to aeration. The numerical methodologies consisted of defining the position where: (iii) the boundary layer thickness (δ) exceeds the equivalent clear-water depth; (iv) the root mean square value of the instantaneous fluctuating wall-normal velocity (u_{rms}), approximated by the value of turbulent kinetic energy (k) close to the free surface, exceeds the effects of surface tension and gravity (Chanson, 1993); and (v) destabilizing energies exceed stabilizing energies per unit volume (Bombardelli et al., 2011).

Tabari & Tavakoli (2016) studied the effects of stepped spillway geometry in energy dissipation along the chute for different discharges, varying quantity, height and length of steps. They used the software FLOW-3D, with free surface treatment with the VOF method and turbulence modeling with the $k-\epsilon$ model. The numerical model validation was done for other geometries, among which that of Felder & Chanson (2011) can be mentioned, from where experimental data of air distribution downstream of the inception point were obtained. It should be pointed out that their validation can be questioned because the physical structure of Felder & Chanson (2011) has a chute with nonuniform step heights with a longitudinal slope of 1V:2H, different from the studied structure with uniform step heights with a slope of 1V:1H.

Toro et al. (2016) characterized the nonaerated region of skimming flow down stepped spillways with OpenFOAM software. The turbulence models used were $k-\epsilon$, RNG $k-\epsilon$ and Lauder-Gibson RSM and the free surface treatment was done using the VOF method. The authors verified that the numerical results are well adjusted to the experimental results obtained with particle image velocimetry (PIV) and that the velocity profiles, turbulent kinetic energy (k) and turbulent kinetic energy dissipation (ϵ) present a similar evolution along the chute. Lopes et al. (2018) sought to establish a procedure for defining the free surface along a stepped chute using the CFD method and the VOF method with the OpenFOAM software and SST $k-\omega$ turbulence model. The authors comment that the correct definition of the free surface of the air-water two-phase flows is not unanimous in the literature. According to Lopes et al. (2018), it is usual to define the free surface

in experimental works by adopting the depth where there is an air concentration equal to 90% (Boes & Hager, 2003; Bung, 2013; Chanson, 1993; Pfister & Hager, 2010a, 2010b), whereas, in the works with numerical approaches with VOF models, or similar, the position of the free surface is usually defined by the equilibrium between the volumes of water and air, that is, for a fraction of water (α) equal to 0.5 (Albadawi et al., 2013; Bombardelli et al., 2011; Daneshfaraz et al., 2016; Toro et al., 2016). In a smaller quantity, some works with a numerical approach consider the same usual criterion of experimental studies, defining the free surface as the depth where the air concentration is equal to 90% (Kositgittiwong et al., 2013; Meireles et al., 2014). Lopes et al. (2018) concluded that there is no global isoline of water fraction (α) that predicts the surface of the flow. Thus, the authors suggest the use of $\alpha = 0.7$ for the nonaerated zone and $\alpha = 0.1$ for the aerated zone, resulting in a 2% error when compared with the experimental results. The consideration of $\alpha = 0.5$ should be done only for the nonaerated zone, where the authors obtained errors between 5 and 8%.

It is observed, therefore, that computational numerical modeling with CFD tools, if used correctly, presents great potential for application in engineering practice in the initial stages of projects and/or in conjunction with physical models (Arantes, 2007; Aydin & Ozturk, 2009, 2010; Chen et al., 2002). Aydin & Ozturk (2010) further comment that these CFD analyses, based on relatively simple mathematical models, are already commonly used in aerodynamic, nuclear, industrial and other models.

This paper, therefore, aims to answer the following scientific questions:

- Are the CFD tools that use RANS techniques suitable for modeling the air-water two-phase flow that occurs on stepped spillways? Are the mean values of pressure and velocity representative when compared with experimental data?
- In physical modeling, the pressure measurement in the steps is made at specific points, and may not necessarily register the extreme mean pressures (positive and negative) that occur in the horizontal and vertical faces of steps. Can CFD be used to investigate measurement effects due to uncertainties in meter position considering a full-scale prototype?

MATERIALS AND METHODS

To answer the two questions, the methodology presented in this paper aims to validate the numerical model, to analyze the behavior of the mean pressures on horizontal and vertical faces of steps and to estimate how far these values distance themselves from the average maximum pressures (horizontal faces) and minimum (vertical faces) that would be measured if, experimentally, the measurement of pressures were continuous along the steps. This methodology is divided into sections dealing with the experimental setup, the numerical modeling, the validation methodology of this numerical model and the data analysis.

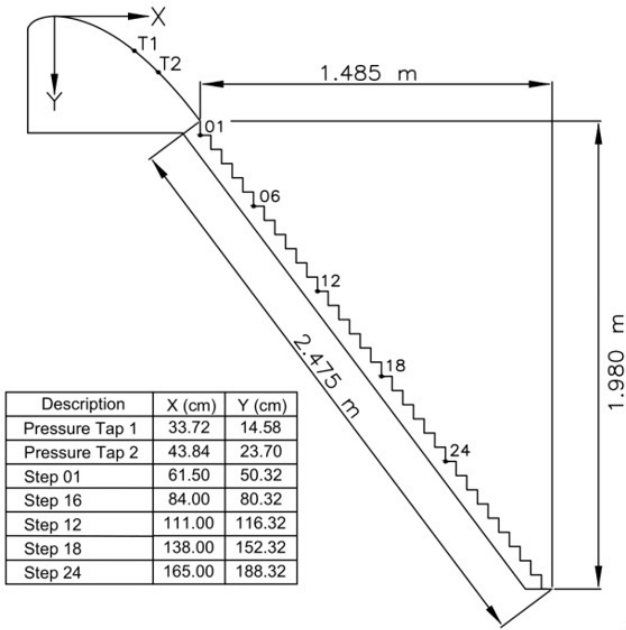
Experimental setup

The physical hydraulic structure used in this work is described in Sanagiotto (2003), Sanagiotto & Marques (2008) and Gomes (2006) and is very similar to the structure used in other studies (Conterato, 2011, 2014; Conterato et al., 2015; Novakoski et al., 2017a, 2017b; Osmar et al., 2018), with small differences in the approach channel and the channel downstream of the steps.

The hydraulic structure (Figure 1) is a physical model scaled 1:10 with a total drop height of 2.44 m and a chute 0.40 m wide with a slope of 1.0V:0.75H (53.13°). The chute is composed



(a)



(b)

Figure 1. Physical model with steps 0.06 m height: (a) photo of the structure during a test and (b) sketch of the structure with coordinates of the pressure taps and external edges of monitored steps (adapted from Sanagiotto, 2003).

of 32 steps, 0.06 m height. The upstream end of the ogee crest is smooth, without variable size steps between the ogee and the chute. The design head is $H_d = 0.40$ m and the ogee profile is described by $Y = 1.08945.X^{1.85}$, with origin on the crest.

Data from Sanagiotto & Marques (2008) and Sanagiotto (2003) include specific discharges between $0.03 \text{ m}^3/\text{s}/\text{m}$ and $0.70 \text{ m}^3/\text{s}/\text{m}$, corresponding to the skimming flow regime. These authors evaluated depths, velocities, average and instantaneous pressures and aeration inception points.

Depths were measured with a point gauge perpendicular to the pseudobottom and in the center of the chute. Mean velocities were measured with a Pitot tube coupled with a differential pressure transducer. Mean and instantaneous pressures were measured with transducers and piezometers at positions distant 0.375 cm, 1.625 cm, 2.875 cm and 4.125 cm from the outer edge at the horizontal faces and distant 0.50 cm, 2.15 cm, 3.80 cm and 5.45 cm from the outer edge in the vertical faces, totaling eight pressure taps on each measured step. Flow aeration evaluations were performed visually. The measurements of pressure, depth and velocity were performed at steps 01, 06, 12, 18 and 24, as shown in Figure 1b.

Different models of pressure transducers were used, with maximum errors of ± 9 mm and minimum of ± 2 mm. The differential transducer used in the velocity measurements had an error of ± 6 mm, resulting in errors in velocity measurements of the order of ± 0.35 m/s. The data were collected at a frequency of acquisition of 50 Hz over a 180 seconds interval. Of the eight pressure taps at steps, six were monitored with transducers and only two with piezometers (close to the inner corner of the step, one in vertical and the other on the horizontal face). For more details, see Sanagiotto (2003), Sanagiotto & Marques (2008) and Gomes (2006).

Conterato et al. (2015) provided pressure data along the same chute used by Sanagiotto & Marques (2008) in all the 20 first steps with only one pressure tap on each vertical and horizontal face, distant 3 mm from the external edge of the steps. The transducers used to obtain this data have maximum errors of ± 9 mm (Conterato, 2011; Gomes, 2006).

Numerical modeling and governing equations

Three-dimensional flow simulations were performed using the Ansys CFX software, which uses the finite volume method (Ansys Inc., 2013) and has a history of successful use for CFD simulations of various hydraulic structures (Arantes, 2007; Arantes et al., 2010; Dettmer et al., 2013; Gabl & Righetti, 2018; Sanagiotto et al., 2019a, 2019b).

The equations of continuity and momentum solved by the software are

$$\frac{\partial \rho}{\partial t} + \frac{\partial (\rho u_j)}{\partial x_j} = 0 \quad (3)$$

$$\frac{\partial \rho u_j}{\partial t} + \frac{\partial (\rho u_i u_j)}{\partial x_j} = -\frac{\partial p'}{\partial x_i} + \frac{\partial}{\partial x_j} \left[\mu_{eff} \left(\frac{\partial u_i}{\partial x_j} + \frac{\partial u_j}{\partial x_i} \right) \right] + S_M \quad (4)$$

where: ρ = fluid density; t = time; $u_{i,j}$ = velocity; p' = modified pressure, given by Equation 5; μ_{eff} = effective viscosity; S_M = some of the body forces (Ansys Inc., 2013); p = pressure; and k = turbulence kinetic energy.

$$p' = p + \frac{2}{3}\rho k \quad (5)$$

The turbulence was modeled in the RANS technique with the turbulence model $k-\epsilon$ (Jones & Launder, 1972; Launder & Spalding, 1974), which has a long history of applications in studies with CFD related to stepped spillways (Aydin & Ozturk, 2009; Bayon et al., 2018; Bombardelli et al., 2011; Chen et al., 2002; Li et al., 2018a; Lobosco & Schulz, 2010; Meireles et al., 2014; Tabari & Tavakoli, 2016; Tabbara et al., 2005; Toro et al., 2016). This model is based on the concept of viscosity within the boundary layer, so that the effective viscosity (μ_{eff}) is the sum of the molecular viscosity (μ) and the turbulent viscosity (μ_t) of the fluid. It is assumed that the turbulent viscosity is related to the turbulent kinetic energy (k) and to the turbulent kinetic energy dissipation rate (ϵ) according to Equation 6, where C_μ is a dimensionless constant and equal to 0.09, in this study. The values of k and ϵ are obtained directly from the differential transport equations.

$$\mu_t = C_\mu \rho \frac{k^2}{\epsilon} \quad (6)$$

The multiphase model adopted was the homogeneous model with a free surface at the interface. According to Stenmark (2013), the homogeneous model implemented in Ansys CFX corresponds to the VOF model, which solves a set of momentum equations in the domain, storing the volume of the two phases in each cell as a fraction (Hirt & Nichols, 1981). In Equations 7 and 8, the physical properties of density (ρ) and viscosity (μ) are obtained in each cell from the volume fractions of air (α_{air}) and water (α):

$$\rho = \alpha \cdot \rho_{water} + \alpha_{air} \cdot \rho_{air} \quad (7)$$

$$\mu = \alpha \cdot \mu_{water} + \alpha_{air} \cdot \mu_{air} \quad (8)$$

Further details can be found at Ansys Inc. (2013).

Boundary conditions

The simulations were carried out for the steady flow regime, with mesh adaptation at the air-water interface and with a high-resolution advection scheme.

Boundary conditions were applied to all faces of the domain shown in Figure 2, as described below. This figure indicates the faces where the conditions inlet, outlet and opening were applied. A non-slip boundary condition was applied to other faces (chute, bottom, approach and restitution channels, and crest) considering a null roughness to all the walls.

The domain of the numerical model has a smaller width than the physical model. So, it was decided to consider the condition of symmetry in the walls of the structure, which forces the variables of field of flow to be mirror images with respect to the field of symmetry (Çengel & Cimbala, 2006). This simplification impairs the representation of anisotropic turbulence, but allows

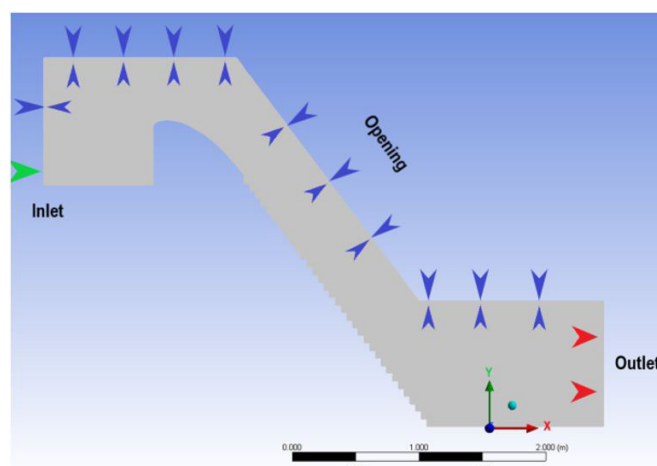


Figure 2. Domain and boundary conditions used in the numerical model.

the reduction of computational effort and eliminates possible wall effects due to the smaller structure width (Arantes, 2007).

For the inlet condition, a mass flow discharge was applied. A high turbulence intensity (10%) was applied in the inlet condition based on Ma et al. (2002), who, when studying an urban river subject to flooding in a mountainous region, observed that the simulated velocities did not present graphically visible differences considering the turbulence intensity in the inlet and outlet conditions as 5%, 10% and 20%, impacting only the magnitude of the turbulent kinetic energy and the rate of dissipation of the flow and only in the region close to the inlet and outlet boundary conditions. In the outlet, atmospheric pressure was applied as a boundary condition. At the top, opening conditions were considered with a high intensity of turbulence (10%) and atmospheric pressure.

Simulated specific discharges were $0.20 \text{ m}^3/\text{s}/\text{m}$ and $0.30 \text{ m}^3/\text{s}/\text{m}$ on a model scale (1:10), equivalent to $6.3 \text{ m}^3/\text{s}/\text{m}$ and $9.5 \text{ m}^3/\text{s}/\text{m}$ on full-scale prototype conditions. It was determined by experimental observations (Sanagiotta & Marques, 2008) that the inception points are located on steps 14 and 21, respectively, for the simulated discharges.

Grid testing and model validation

The grid testing was made with the Grid Convergence Index (GCI) method, presented by Celik et al. (2008) and proposed initially by Roache (1994), which allows estimation of the uncertainties arising from the use of a given grid for any variable. After the grid definition, the model validation was developed by comparing experimental data and numerical results.

The GCI method was developed based on the Richardson extrapolation aiming to provide an objective asymptotic approximation to quantify the uncertainty of the grid convergence. This method has a history of application in studies with CFD simulations in spillway structures (Aydin & Ozturk, 2009; Bai et al., 2017; Bayon et al., 2018; Li et al., 2018b; Lopes et al., 2018; Teng & Yang, 2016; Yang et al., 2019).

In general terms, in an analysis of three meshes with different numbers of elements, if the uncertainties due to the grid convergence, quantified numerically as the GCI, are lower

than the accuracy of the measurement of a variable, such as pressure or velocity, the intermediate mesh can be chosen. A more refined mesh would require more computational effort and the increase of precision would not be justified in comparison with measurement errors.

The GCI was calculated for mean pressures close to the external edges of the steps, distant 0.375 cm from these, in agreement with the experimental apparatus of Sanagiotto & Marques (2008). Three simulations were performed with the same contour and flow conditions, with three unstructured meshes (Figure 3) with mesh adaptation at the air-water interface. The numbers of elements of the meshes at the beginning of the simulation were 3.7×10^5 (coarse grid), 1.1×10^6 (medium grid) and 3.1×10^6 (fine grid).

A widely used methodology for the validation of numerical models is the visual comparison between physical and numerical model data of depths (Chen et al., 2002; Tabbara et al., 2005), velocities (Arantes, 2007; Bombardelli et al., 2011; Chen et al., 2002) and pressures (Arantes, 2007; Chen et al., 2002) or even in visual comparison on a prototype scale of these variables (Araújo Filho & Ota, 2016). In the present work, this validation was carried out from data of mean pressure (Conterato et al., 2015) and velocity data found in the literature (Amador et al., 2009; Boes & Hager, 2003; Meireles et al., 2012; Tozzi, 1992; Zhang & Chanson, 2016a).

Data analysis

To establish a procedure to determine the free surface of the skimming flow for spillways with slope of 1V:0.75H from CFD simulations using the VOF method, or similar, depth data were used (Sanagiotto, 2003) to establish values of the fraction of water (α) that describe the free surface of the flow, such as done by Lopes et al. (2018).

The velocities obtained numerically were used to adjust a power-law velocity profile expressed by Equation 9 for the boundary

layer development in the nonaerated region. The adjustment coefficient ($1/N$) serves as a parameter of validation of the numerical model through comparison with values presented in the literature (Amador et al., 2009; Bombardelli et al., 2011; Meireles et al., 2012; Zhang & Chanson, 2016a). For the aerated region of the flow, the power law to be adjusted is expressed by Equation 10 (Boes & Hager, 2003; Chanson, 1994), where the dimensionless variable of the x-axis is related to the flow depth (h_{90}), and not to the thickness of the boundary layer (δ).

$$\frac{u}{u_{max}} = \left(\frac{y}{\delta}\right)^{1/N} \quad (9)$$

$$\frac{u}{u_{90}} = \left(\frac{y}{h_{90}}\right)^{1/N} \quad (10)$$

where: u = longitudinal velocity; y = normal distance to the pseudobottom; δ = boundary layer thickness; N = exponent; h_{90} = characteristic mixture (air-water) depth with local air concentration of $C = 0.90$; u_{max} = free-stream velocity; and u_{90} = mixture surface velocity (velocity at the depth h_{90}).

To analyze the effect of possible errors of measurement of extreme pressures commonly adopted in projects ($P_{0.1\%}$ and $P_{99.9\%}$), due to the uncertainties in the position of the transducer in the steps, experimental data of pressure measured with transducers by Sanagiotto & Marques (2008) were used in this study. The standard deviation values (σ_d) and statistical probability distribution coefficients $N_{0.1\%}$ and $N_{99.9\%}$ were calculated, respectively, using Equations 11 and 12, following the same methodology used in studies of extreme pressures in hydraulic jumps (Novakoski et al., 2017b; Teixeira, 2008).

$$N_{0.1\%} = (P - P_{0.1\%}) / \sigma_d \quad (11)$$

$$N_{99.9\%} = (P_{99.9\%} - P) / \sigma_d \quad (12)$$

where: $P_{\%}$ = pressure head with a certain probability of nonexceedance. These parameters were used to transform values of mean pressure heads (P), obtained numerically, into $P_{0.1\%}$ and $P_{99.9\%}$.

The effects of the uncertainties in the maximum and minimum mean pressures were analyzed at extreme pressures ($P_{0.1\%}$ and $P_{99.9\%}$), on a prototype scale, due to the position of the transducers and piezometers.

MODEL VALIDATION

The model validation was carried out from data of mean pressure and velocity data found in the literature. However, to define the velocity profiles, it was necessary to establish a procedure to determine the free surface of the skimming flow, as shown in the following sections.

Grid testing and model validation through mean pressure

The calculated pressures in the two first steps showed to be very sensitive to the mesh size, well beyond the sensitivity observed in the rest of the chute. The possible cause is the

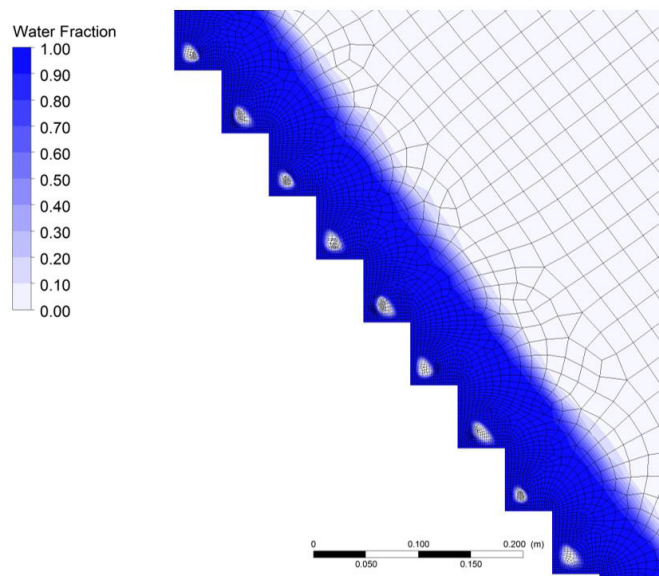


Figure 3. A medium grid in the region on the first steps of the stepped spillway and the water fraction (α) at the end of the simulation.

abrupt change of the flow surface (Bindo et al., 1993) because there are no transitional steps in the experimental model nor in the numerical model. Thus, for the mesh definition study, it was decided to disregard steps 1 and 2, understanding that from step 3 the uncertainties due to the mesh reduce significantly and assume a more homogeneous and adequate behavior for the proposed analysis.

The uncertainty due to the mesh in the values of mean pressure at the horizontal faces, considering the region close to the external edge of 18 consecutive steps (steps 3 to 20, due to the availability of experimental data) ranged from 0.61% to 7.06%, with an average value of 3.77%, lower than the uncertainty of 5.4% estimated for pressures in Bai et al. (2017) for similarly analyzed steps. For the pressures in the vertical faces, the uncertainty in the average pressure due to the mesh, in the region near the external edge, ranged from 0.01% to 5.08%, with an average value of 1.87%.

Figure 4 shows the development of pressure head profiles at the horizontal faces along the chute, between steps 10 and 20, using the three meshes for the grid testing, and Figure 5 shows the results using only the medium grid and the pressure head values obtained experimentally (Conterato et al., 2015) 3 mm from the external edge of each step for the model validation.

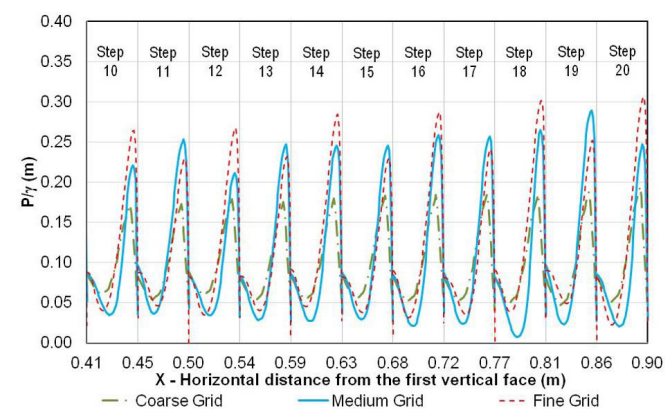


Figure 4. Pressure heads at the horizontal faces along the chute, between steps 10 and 20: simulations' results for the grid testing, for the specific discharge $q = 0.30 \text{ m}^3/\text{s}/\text{m}$.

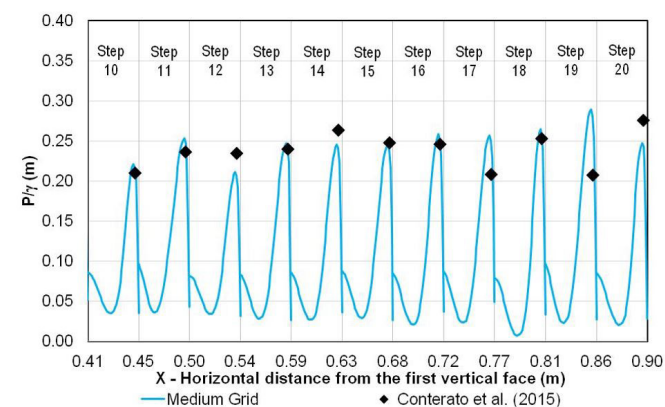


Figure 5. Pressure heads at the horizontal faces along the chute, between steps 10 and 20: simulations' results with medium grid and experimental data for the model validation ($q = 0.30 \text{ m}^3/\text{s}/\text{m}$); in the model scaled 1:10.

As shown in Figure 5, the maximum values obtained numerically for the intermediate mesh, for example, are either larger or smaller than the experimental values for different steps. It is also observed that the position of the experimental pressure tap (transducer) is slightly to the right of the position of the maximum pressure in some steps. Thus, it was considered that the numerical model is able to represent the experimentally obtained pressures in most of the steps, considering that small errors in the relative position of the transducer (x/l) could justify greater differences between the experimental pressures and the simulations' results.

When comparing the numerical and experimental data of pressure heads in the same relative position of the horizontal faces (at 3 mm of the outer corner of each step), a mean difference of 1.6% was obtained, with root mean square error (RMSE) equal to 0.03 m for steps 3 to 20.

Similarly, Figure 6 shows the development of pressure head profiles in the vertical faces along the chute, between steps 10 and 20, using the three meshes for the grid testing, and Figure 7 shows the results using only the medium grid and the experimental data (Conterato et al., 2015), also obtained 3 mm from the outer corner of each step for the model validation.

Compared with the results obtained for the horizontal faces, bigger differences in the vertical faces between the extreme pressure heads obtained numerically and experimentally were observed. However, it is observed that the profiles of pressure heads in the vertical faces are quite accentuated so that at small vertical distances in the vertical faces there is a significant increase in the magnitude of the pressures. In step 17, for example, considering the medium grid, in a space of 3 mm, the pressure head goes from 0 to $-0.067 \text{ mH}_2\text{O}$ (minimum profile value), so that more extreme pressures may not have been recorded in the experiments because the position of the transducer did not match where the most extreme pressure occurred.

Furthermore, considering the error of $0.009 \text{ mH}_2\text{O}$ for transducers, more significant percentage errors in the vertical

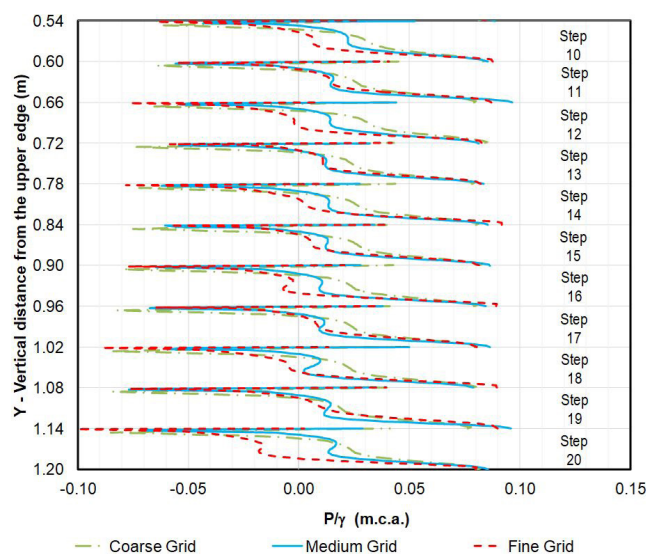


Figure 6. Pressure heads at the vertical faces along the chute, between steps 10 and 20: simulations' results for the grid testing, for the specific discharge $q = 0.30 \text{ m}^3/\text{s}/\text{m}$.

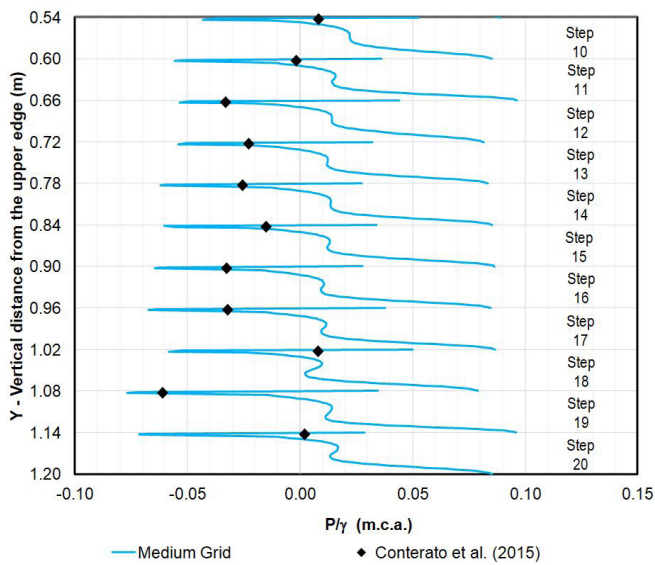


Figure 7. Pressure heads at the vertical faces along the chute, between steps 10 and 20: simulations’ results with medium grid and experimental data for the model validation ($q = 0.30 \text{ m}^3/\text{s}/\text{m}$); in the model scaled 1:10.

faces are expected because the magnitude of the pressure heads is lower than in the horizontal faces. When comparing the experimental data with the pressure heads obtained numerically in the same position in the vertical faces (at 3 mm of the outer corner of the step), there is an average difference equal to 5.8%, with $\text{RMSE} = 0.04 \text{ m}$, considering steps from 3 to 20.

From the maximum errors of $\pm 0.009 \text{ m}$ characteristic of the transducers, average errors of 3.84% for the pressures at the horizontal faces and 41.84% for the pressures in the vertical faces were calculated for the experimental data. Because the value of the mean pressures in the vertical faces is relatively low, the error resulted in a large value (41.84%). Because the pressure measurement error is greater than the uncertainty due to the grid convergence, quantified numerically as the GCI, it was decided to use the medium grid with 1.1×10^6 elements, considering an uncertainty due to the mesh size of 3.77% for the pressures at the horizontal faces and 1.87% for the pressures in the vertical faces.

Procedure for determining the free surface of the flow along the stepped spillway

For the determination of the free surface of the air-water two-phase flow, experimental data (Sanagiotto & Marques, 2008) and numerical values of dimensionless depths (h/h_c) were compared along the chute (x/x_i), according to Figure 8, where x = horizontal distance from the vertical face of the first step and x_i = position of the inception point. The depths obtained numerically from the corner of each step and perpendicular to the pseudobottom are presented for different water fractions (α), so that $\alpha = 0.1$ indicates the depth where there is 10% water and 90% air, for example, and $\alpha = 0.5$ indicates the depth where there is equilibrium between air and water along the section analyzed.

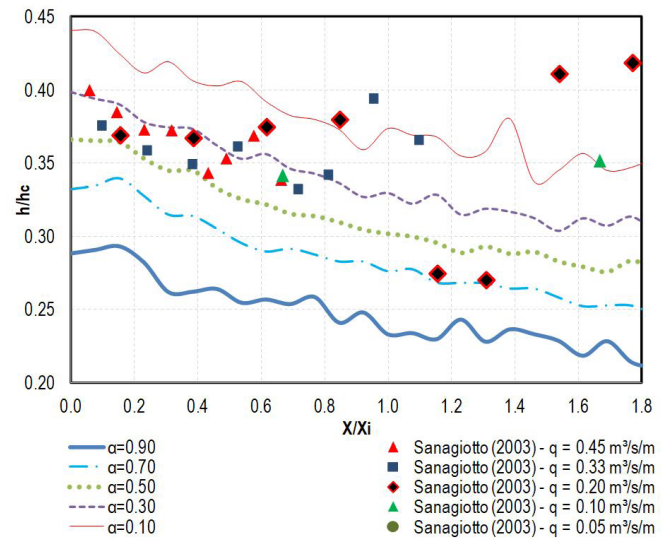


Figure 8. Mean depths obtained experimentally and isolines of mean depths obtained numerically for the specific discharge $q = 0.20 \text{ m}^3/\text{s}/\text{m}$ for water fraction values from $\alpha = 0.90$ to $\alpha = 0.10$ along steps 01 to 25.

For the nonaerated region of the flow ($0 \leq x/x_i \leq 1$), the experimental data of depths are close to the isoline $\alpha = 0.30$. Considering the experimental depths for the specific discharge $q = 0.20 \text{ m}^3/\text{s}/\text{m}$, the errors calculated for the isoline $\alpha = 0.30$ vary between 13% and 2%, with an average of 7%, which represents a mean error equal to 4 mm.

For the aerated region of the flow ($x/x_i > 1$), there are less experimental data for the evaluation of which isoline best represents the observed free surface. However, there is an indication that the water fraction is less than $\alpha = 0.30$ because there are two points exactly on the isoline $\alpha = 0.10$, two points above this value and two points near the isoline $\alpha = 0.70$. When considering the depths for the specific discharge $q = 0.20 \text{ m}^3/\text{s}/\text{m}$, the errors calculated for the isoline $\alpha = 0.10$ vary between 34% and 16%, with an average of 25%, which represents a mean error equal to 13 mm. Although these errors are significant, observing physical models of spillways in laboratories, an absolute error of 13 mm in the aerated region of the skimming flow can be accepted due to the great oscillation of the depths during the tests.

Different from the usual consideration in CFD simulations where the free surface is determined from the isoline where there is the balance between water and air $\alpha = 0.50$ (Albadawi et al., 2013; Bombardelli et al., 2011; Daneshfaraz et al., 2016; Toro et al., 2016) and based on the hypothesis of Lopes et al. (2018) that there is no global isoline of water fraction that predicts the free surface at all flows down stepped spillways, different isolines of α were determined for the aerated and nonaerated regions of the flow. So, for spillways with slopes of 1V:0.75H, it is recommended to use $\alpha = 0.30$ for the nonaerated region and $\alpha = 0.10$ for the aerated region.

Although greater differences were found between the experimental and numerical results for the aerated region, the use of $\alpha = 0.10$ has physical sense, so that many experimental studies

in the aerated region consider the depth to be h_{90} (Boes & Hager, 2003; Bung, 2013; Frizell & Frizell, 2015; Meireles et al., 2014).

There are descriptions in the literature of homogeneous multiphase models being considered adequate to evaluate a series of skimming flow characteristics in stepped spillways, such as velocities, pressures and depths (Bai et al., 2017; Bai & Zhang, 2017; Bombardelli et al., 2011; Daneshfaraz et al., 2016; Kositgittiwong et al., 2013; Lopes et al., 2018). However, when the analysis is associated with the air entrainment into the flow, the multiphase model configurations are still being discussed. There are papers that consider that the homogeneous multiphase model is adequate to analyze air incorporation (Arantes, 2007; Zhan et al., 2016) and other works have shown that there are more adequate models (Van Alwon et al., 2017, 2019). Thus, the procedure proposed here for determining the free surface of the flow along the stepped spillway is limited to simulations with homogeneous multiphase models, such as described in the methodology of the present work.

Validation through velocity distribution

Velocity profiles normalized by u_{max} inside the boundary layer in the nonaerated region (steps 3 to 14, for $q = 0.20 \text{ m}^3/\text{s}/\text{m}$) obtained from numerical results were adjusted to a power law, according to Equation 9, with exponent $N = 3.9$ ($R^2 = 0.87$), as shown in Figure 9.

The value found for the exponent, $N = 3.9$, is closer to the exponent found in other studies performed for the nonaerated region with experimental approaches, where Zhang & Chanson (2016a) obtained the exponent $N = 4.5$ in a model with slope of 1.0V:1.0H, Meireles et al. (2012) obtained $N = 3.4$ for a stepped spillway with a slope of 1.0V:0.75H and Amador et al. (2009) obtained $N = 3.0$ for a similar structure with a slope of 1.0V:0.8H.

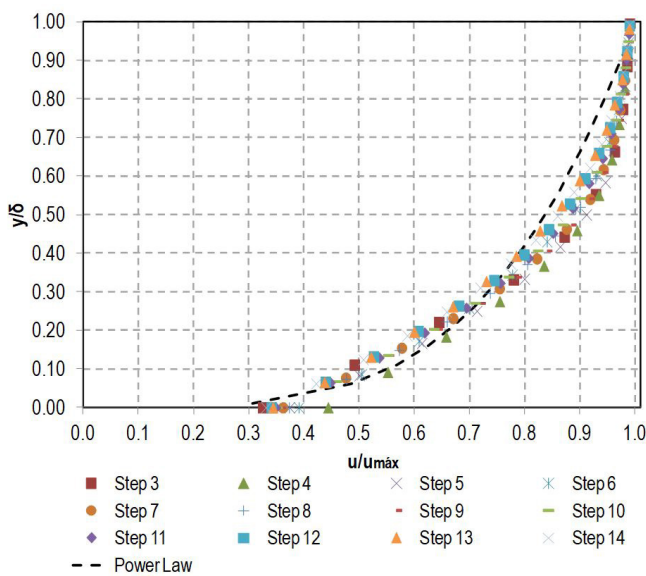


Figure 9. Velocity profiles from numerical results in the development of the boundary layer in the outer corners of steps 3 to 14 and profile adjusted with a power law with exponent $N = 3.9$ for a specific discharge $q = 0.20 \text{ m}^3/\text{s}/\text{m}$.

From a numerical approach, similar to what is presented in the present work, Bombardelli et al. (2011) calculated an exponent $N = 5.4$ for the nonaerated region of the skimming flow down a stepped spillway with a slope of 1.0V:0.75H.

For the aerated region (steps 15 to 25, for $q = 0.20 \text{ m}^3/\text{s}/\text{m}$), velocity profiles were related to the characteristic depth h_{90} and normalized by u_{90} , according to Equation 10 and Figure 10. These profiles were adjusted to a power law with $N = 3.5$ and with an adjustment coefficient equal to 1.05, similar to the equation of Boes & Hager (2003), who obtained an exponent $N = 4.3$. Equation 13 express the power-law velocity profile ($R^2 = 0.92$).

$$\frac{u}{u_{90}} = 1.05 \left(\frac{y}{h_{90}} \right)^{1/3.5} \quad (13)$$

If the coefficient of adjustment is disregarded, the exponent becomes $N = 4.0$, as shown in Equation 14 ($R^2 = 0.89$). The value of $N = 4.0$ is equal to that suggested by Chanson (1994) for the data presented in Tozzi (1992) for a chute with a slope of 1.0V:0.75H.

$$\frac{u}{u_{90}} = \left(\frac{y}{h_{90}} \right)^{1/4.0} \quad (14)$$

RESULTS AND DISCUSSION

Mean pressures on the surfaces of the steps

In the present study, numerical results of mean pressure profiles were normalized by maximum mean pressure along each horizontal face (Figure 11). The mean pressure profile (dashed line) was constructed only from numerical data as the mean of the normalized pressures of steps 3 to 21. It was observed that the relative position of the maximum mean pressure occurs

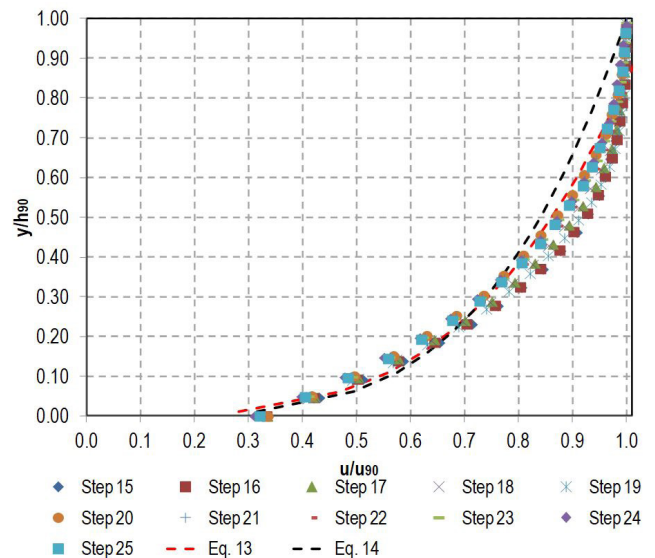


Figure 10. Velocity profiles from numerical results in the aerated region (steps 15 to 25, for $q = 0.20 \text{ m}^3/\text{s}/\text{m}$) in the outer corners and profiles adjusted with power laws.

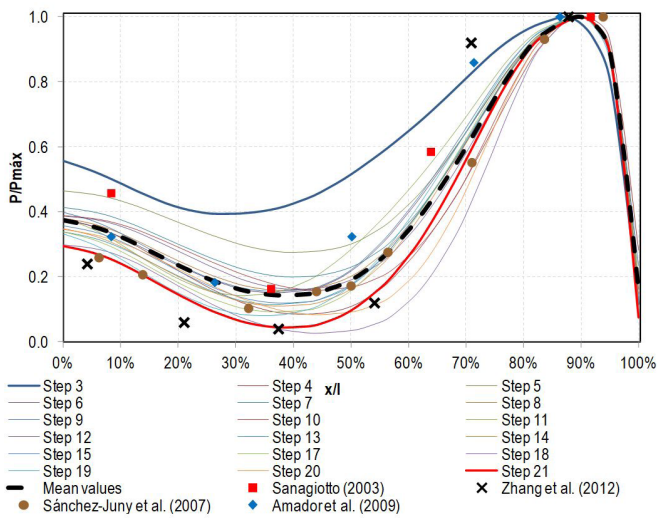


Figure 11. Nondimensional pressure profiles (P/P_{max}) for different relative positions (x/l) along the horizontal faces of steps in the nonaerated region (steps 3 to 21), the average mean pressure profile from numerical results with $q = 0.30 \text{ m}^3/\text{s}/\text{m}$ and experimental data found in the literature.

between $x/l = 85\%$ and $x/l = 92\%$, where x = horizontal distance from the vertical face to a given point and l = length of the step. In this figure it was included literature experimental data obtained in horizontal faces of steps: Sanagiotto (2003) at steps 6, 12, 18 and 24, for $q = 0.33 \text{ m}^3/\text{s}/\text{m}$ and a chute with a slope of 1.0V:0.75H; Sánchez-Juny et al. (2007) and Amador et al. (2009) for $q = 0.33 \text{ m}^3/\text{s}/\text{m}$ and a chute with a slope of 1.0V:0.8H, at the aerated region; and Zhang et al. (2012) for $q = 0.23 \text{ m}^3/\text{s}/\text{m}$ and a chute with a slope of 1.0V:2.0H, also in the aerated region.

It was considered that in the experimental data obtained from the literature (Figure 11), the position of the transducer or piezometer was able to measure the maximum pressure (i.e., it is possible to observe the point where $P/P_{max} = 1.0$ happens).

By analyzing the relative positions of the pressure points of the cited studies, it can be seen that the positions of the points closest to the outer corners of the horizontal faces vary from $x/l = 86\%$ (Amador et al., 2009) to $x/l = 94\%$ (Sánchez-Juny et al., 2007). From the mean pressure profile (dashed line of Figure 11), the pressures at these positions could correspond to the dimensionless pressures $P/P_{max} = 0.98$ and $P/P_{max} = 0.93$, respectively.

In addition, pressure profiles were normalized by the minimum mean pressure along the vertical faces, as shown in Figure 12, where there are also experimental data presented in the literature (Sanagiotto, 2003; Sánchez-Juny et al., 2007). It was observed that the relative position of the minimum pressure occurs between $y/h = 94\%$ and $y/h = 98\%$. As indicated in Figure 12, the applied numerical model showed negative pressures in the vertical faces more extreme than those obtained experimentally in all the steps. Differences such as these, to a greater or lesser extent, have already been presented in other works, such as in Chen et al. (2002) and Arantes (2007), where the authors validated numerical models and showed results with negative pressures from numerical results more extreme than those measured experimentally.

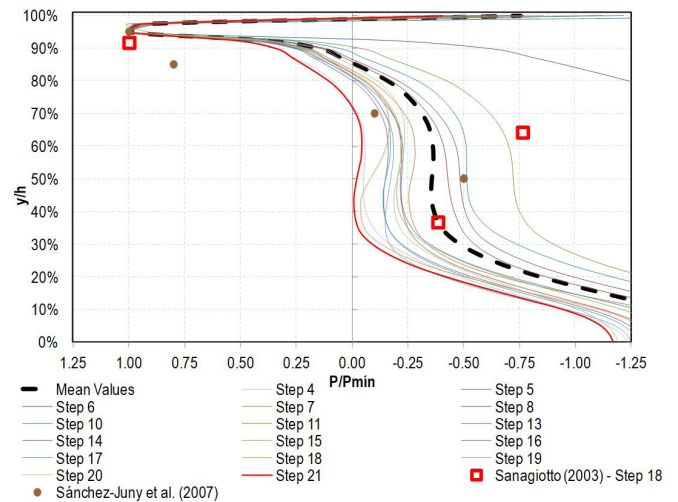


Figure 12. Nondimensional pressure profiles (P/P_{min}) for different relative position (y/h) along the vertical faces of steps in the nonaerated region (steps 4 to 21), the average mean pressure profile from numerical results with $q = 0.30 \text{ m}^3/\text{s}/\text{m}$ and experimental data found in the literature.

Figure 12 shows that along most of the surface of the vertical faces there are no negative pressures and even positive pressures have small magnitude and are therefore subject to greater relative errors due to the accuracy of the measuring equipment.

Nonetheless, it is observed that the pressure gradients are bigger in the upper part of the vertical face, compared with that observed in the horizontal faces. For example, when the region of $0.85 < y/h < 0.95$ is analyzed, the pressure starts from a zero value until it reaches its minimum value. This variation happens in 5 mm or 6 mm for a model with steps 5 cm height (Amador et al., 2009) or 6 cm height (Sanagiotto & Marques, 2008; Zhang et al., 2012), respectively, which are small distances. As a result, it is difficult to state that the experimental records on the vertical faces of the steps represent the minimum pressures occurring at the top of the step because these recorded values are sensitive to the relative position of the transducers and piezometers.

Statistical parameters of pressures with different probabilities of being overcome on the surfaces of the steps

As a result of steady flow simulations, mean pressures were obtained. However, damage to hydraulic structures can occur due to pressures with greater magnitude and different probability of being exceeded, so that it becomes important to know the extreme pressures and not just the mean values. Pressures with a 0.1% probability of being exceeded by more negative values ($P_{0.1\%}$) (Lopardo et al., 2004) are important to evaluate possible cavitation damage in the vertical faces of the steps; and extreme positive pressures, for example, with a 99.9% probability of being exceeded by more positive values ($P_{99.9\%}$) are used for analysis at the horizontal faces (Gomes, 2006).

Experimental data from Sanagiotto & Marques (2008) were used to estimate the statistical coefficients of probability distribution ($N_{0.1\%}$ and $N_{99.9\%}$) as described in Section 2.5 (Equations 11 and 12). These statistical coefficients were used to predict extreme pressures ($P_{0.1\%}$ and $P_{99.9\%}$) through mean pressures (P) obtained in numerical simulations.

Figure 13 shows the statistical probability distribution coefficients for three positions in the vertical faces and three positions in the horizontal faces.

In the vertical faces, at the pressure measured closest to the minimum pressure ($y/h = 92\%$), the values of $N_{0.1\%}$ ranged from 3.46 to 4.48, with an average value of 4.1. The variation of these values was higher in the intermediate position ($y/h = 64\%$) and smaller in the position closest to the internal edge of the step ($y/h = 37\%$).

On the horizontal faces of steps, the maximum values of $N_{99.9\%}$ were observed in the position closest to the center ($x/l = 64\%$), with a maximum value of 4.67. In the pressure measured nearest to the external edge of the step, where the most extreme medium pressures are expected, a maximum value of $N_{99.9\%}$ equal to 3.97 was obtained. From this, Table 1 presents suggested mean values, based on these results, for $N_{0.1\%}$ and $N_{99.9\%}$ for different relative positions of the vertical and horizontal faces, respectively.

Analyzing the values of the standard deviation of the pressure data, it was decided to separate the results for the nonaerated and aerated regions searching for a smaller dispersion of these values.

Figure 14a shows the values of standard deviation (σ_d) normalized by the critical depth (h_c) in the nonaerated region of the flow, whereas Figure 14b presents these values for the aerated region, both along the vertical faces, for different relative positions (y/h).

For the nonaerated region of the flow, where there is a special interest in the extreme pressures for the study of damage due to cavitation (Amador et al., 2009), the results suggest the adoption of the value $\sigma_d/h_c = 0.50$ for the region near the outer corner on the step, where negative pressures occur. For the aerated region of the flow, the dispersion between the values of standard deviation is greater, preventing a unique value being used to obtain pressures with different probabilities from the mean pressures.

Similarly, Figure 15a presents the normalized standard deviation values (σ_d/h_c) in the nonaerated region, while Figure 15b presents these values in the aerated region, both along the horizontal faces for different relative positions (x/l).

In the pressure tap near the external edge of the step, where the most extreme pressures occur at the horizontal faces, the deviation value σ_d/h_c varies between 0.68 and 1.48, with an average of 1.1. In the aerated region, in the same region of the step, the value of the deviation σ_d/h_c varies between 1.09 and 1.62, with an average value equal to 1.4. Thus, similar to that observed

Table 1. Mean values of probability distribution coefficients ($N_{0.1\%}$ and $N_{99.9\%}$) defined based on the experimental data of Sanagiotto & Marques (2008).

Vertical face		Horizontal face	
relative position	$N_{0.1\%}$	relative position	$N_{99.9\%}$
(y/h)		(x/l)	
92%	4.1	92%	3.6
64%	3.8	64%	4.0
37%	3.5	36%	3.7

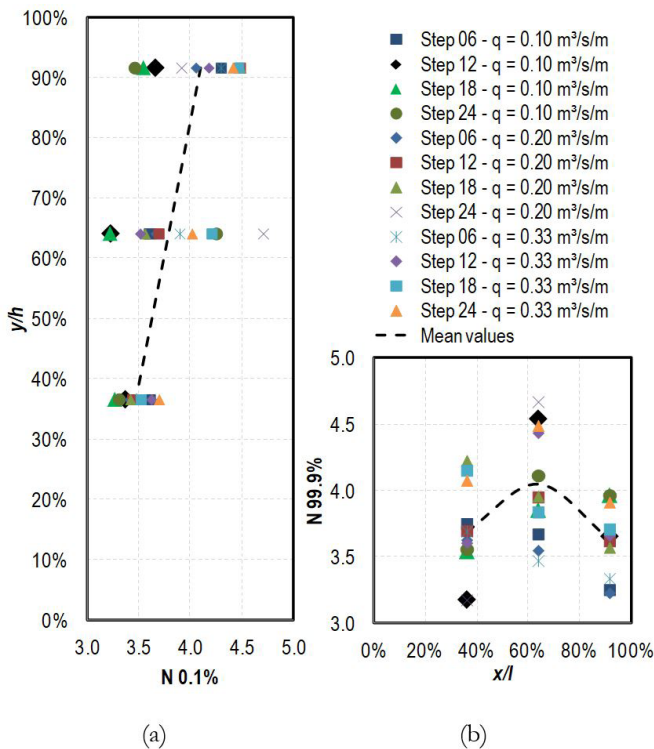


Figure 13. Probability distribution coefficients ($N_{0.1\%}$ and $N_{99.9\%}$) in steps 6, 12, 18 and 24 for different relative positions (a) in the vertical faces (y/h) and (b) in the horizontal faces (x/l), obtained from the experimental data of Sanagiotto & Marques (2008).

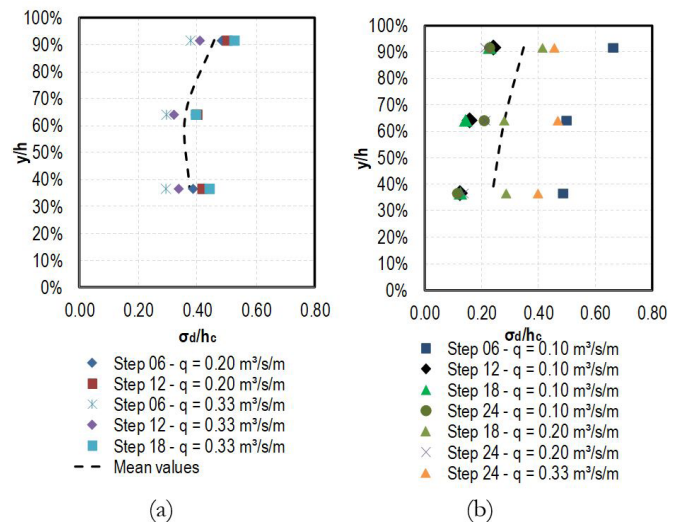


Figure 14. Standard deviation values for instantaneous pressures along the vertical faces obtained from the experimental data of Sanagiotto & Marques (2008) in the (a) nonaerated region and (b) aerated region.

for the standard deviation values in the vertical faces, there is greater dispersion between the instantaneous pressures at the horizontal faces in the aerated region of the flow.

Analysis of uncertainties in pressure data and their implications

To analyze the uncertainties in the pressure data and their implications for the design of stepped spillways, the experimental pressure data of Sanagiotto & Marques (2008), Amador et al. (2009) and Sánchez-Juny et al. (2007) were analyzed for $q = 0.33 \text{ m}^3/\text{s}/\text{m}$ ($h_c = 0.223 \text{ m}$).

Following hypotheses were considered:

- (i) The ratio of mean pressure and maximum mean pressure (P/P_{max}) is distributed along the horizontal faces of the steps according to the profile shown in the dashed line in Figure 11 and the ratio of mean pressure and minimum mean pressure (P/P_{min}) is distributed along the vertical

faces according to the profile shown in the dashed line in Figure 12;

- (ii) The probability distribution coefficient $N_{0.1\%}$ for the region near the outer corner of the vertical faces is equal to 4.1, while the coefficient $N_{99.9\%}$ for the region close to the external corner of the horizontal faces is equal to 3.6;
- (iii) The normalized standard deviation values (σ_d/h_c) were considered differently for vertical and horizontal faces in the nonaerated region ($\sigma_d/h_c = 0.5$ and $\sigma_d/h_c = 1.1$, respectively) and aerated region ($\sigma_d/h_c = 0.4$ and $\sigma_d/h_c = 1.4$, respectively), for the pressure values close to the outer corner of the steps;
- (iv) The pressure data used in this uncertainty analysis were transposed to full-scale prototype conditions by considering the Froude law of similarity and a model scaled 1:10;
- (v) The values of extreme pressure were calculated according to Equations 11 and 12.

Tables 2 and 3 present the calculated values of extreme and mean pressure for vertical and horizontal faces, respectively, for the region near the outer corner of the steps. The presented values are all on a full-scale prototype.

In the first line of Table 2, analyzing the data of Amador et al. (2009) for a vertical face in the aerated region, where the minimum mean pressure experimentally obtained is $P = -0.07 \text{ mH}_2\text{O}$, an extreme pressure $P_{0.1\%} = -3.73 \text{ mH}_2\text{O}$ was calculated, from the assumptions considered and from Equation 11. Because the position of this pressure measurement is $y/h = 93.2\%$, the mean pressure can be corrected by the factor 0.59, from the dashed line of Figure 12, resulting in $P = -0.12 \text{ mH}_2\text{O}$, which would result in a corrected extreme pressure $P_{0.1\%} = -3.78 \text{ mH}_2\text{O}$. However, even though the mean experimental pressure obtained may be 59% of the maximum mean pressure in the vertical face when estimating the extreme pressure $P_{0.1\%}$, no significant differences are observed due to the magnitude of the fluctuation pressure portion. So, the uncertainties in obtaining the mean pressures due to the position of the pressure measurement, in this case, would not result in important errors in the study of cavitation in the vertical faces of the steps in engineering projects.

The same analysis was performed for the vertical face of a step in the aerated region whose mean pressure data are presented

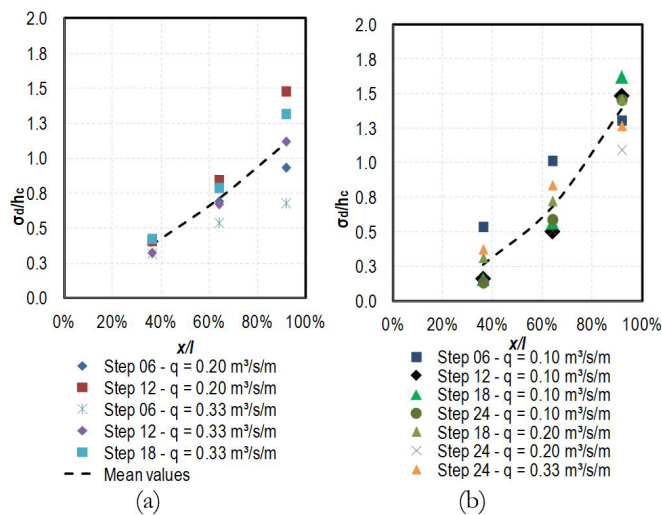


Figure 15. Standard deviation values for instantaneous pressures along the horizontal faces obtained from the experimental data of Sanagiotto & Marques (2008) in the (a) nonaerated region and (b) aerated region.

Table 2. Mean and extreme pressures in full-scale prototype conditions in the region near the external corner of vertical faces from data found in the literature.

Author*, analyzed region**	Mean pressure (mH ₂ O)	σ_d (mH ₂ O)	$N_{0.1\%}$	$P_{0.1\%}$ (mH ₂ O)	Relative position (y/h)	Correction at mean pressure (Figure 12)	Corrected mean pressure [2]/[7] (mH ₂ O)	Corrected $P_{0.1\%}$ (mH ₂ O)	Ratio [9]/[5]
[1]	[2]	[3]	[4]	[5]	[6]	[7]	[8]	[9]	[10]
[a], VFAR	-0.07	0.893	4.1	-3.73	93.2%	0.59	-0.12	-3.78	1.01
[b], VFAR	-0.10	0.893	4.1	-3.76	95.0%	0.99	-0.10	-3.76	1.00
[c], VFAR	-0.23	2.455	4.1	-4.80	91.7%	0.22	-1.05	-5.62	1.17
[c], VFAR	-0.41	0.893	4.1	-4.07	91.7%	0.22	-1.86	-5.52	1.36

* [a] Amador et al. (2009); [b] Sánchez-Juny et al. (2007); [c] Sanagiotto (2003); ** VFAR = vertical face in the aerated region; VFAR = vertical face in the nonaerated region.

Table 3. Mean and extreme pressures in full-scale prototype conditions in the region near the external corner of horizontal faces from data found in the literature.

Author*, analyzed region**	Mean pressure (mH ₂ O)	σ_d (mH ₂ O)	$N_{99.9\%}$	$P_{99.9\%}$ (mH ₂ O)	Relative position (x/l)	Correction at mean pressure (Figure 11)	Corrected mean pressure [2]/[7] (mH ₂ O)	Corrected $P_{99.9\%}$ (mH ₂ O)	Ratio [9]/[5]
[1]	[2]	[3]	[4]	[5]	[6]	[7]	[8]	[9]	[10]
[a], HFAR	2.49	3.124	3.6	13.73	86.3%	0.98	2.54	13.78	1.00
[b], HFAR	2.90	3.124	3.6	14.15	93.8%	0.93	3.12	14.37	1.02
[c], HFNAR	2.75	2.455	3.6	11.59	91.7%	0.98	2.81	11.64	1.00
[c], HFAR	2.59	3.124	3.6	13.84	91.7%	0.98	2.64	13.89	1.00

* [a] Amador et al. (2009); [b] Sánchez-Juny et al. (2007); [c] Sanagiotta (2003); ** HFAR = horizontal face in the aerated region; HFNAR = horizontal face in the nonaerated region.

in Sánchez-Juny et al. (2007). Although the minimum mean pressure in the vertical faces could be corrected by the factor 0.93, due to its relative position and according to the normalized mean pressure profile (Figure 12), no significant differences were observed for the values of $P_{0.1\%}$ with and without the suggested correction. In relation to data presented in Sanagiotta (2003), differences found for the values of $P_{0.1\%}$ were more important. Because the relative position of the pressure measurement closest to the external edge of the step is $y/h = 91.7\%$, and therefore furthest from the region $0.94 < y/h < 0.98$, where the minimum mean pressures were numerically observed, the hypotheses considered suggest that the mean pressure should be corrected by the factor 0.22. This correction resulted in differences in values of $P_{0.1\%}$ equal to 17% and 36%, respectively, for step 18 in the nonaerated region and for step 24 in the aerated region. These differences are, on a full-scale prototype, equal to 0.82 mH₂O and 1.45 mH₂O, which may be important in a cavitation study.

This analysis suggests that when using minimum pressure data on vertical faces of stepped spillways with a slope of 1V:0.75H, attention should be paid to the relative position of the pressure measurement. It should be positioned in the region $0.93 < y/h < 0.98$, so that when using the value of $P_{0.1\%}$, uncertainties in the mean pressure values become less representative in this range.

As shown in Figure 11, the region at the horizontal face where $P/P_{max} > 0.90$ is $0.81 < x/l < 0.98$, being usually the presence of piezometers and transducers in this region in experimental works on stepped chutes, as presented in Table 3. Thus, the uncertainties in the mean pressures due to the position of the pressure measurement are negligible when using values of $P_{99.9\%}$ for projects of stepped spillways.

CONCLUSIONS

In this work, CFD was used to model the air-water two-phase flow down a stepped spillway with a slope of 1.0V:0.75H. The choice of the mesh to be used in the simulations was made by calculating the GCI (Celik et al., 2008) for mean pressures so that the uncertainties due to the grid convergence are lower than the accuracy of the measuring instruments.

It was considered that the computational model was able to adequately reproduce the mean pressures obtained experimentally

(Conterato et al., 2015) for the region near the outer corner of some steps so that some differences can possibly be explained due to the uncertainties about the relative positions of pressure gauges inside the steps. These uncertainties were the subject of a specific study, where mean profiles of pressures normalized by maximum pressure (P/P_{max}) for horizontal faces (Figure 11) and by minimum pressures (P/P_{min}) for vertical faces (Figure 12) were defined.

For the definition of the free surface of the flow, contrary to the criterion usually adopted in CFD studies (Albadawi et al., 2013; Bombardelli et al., 2011; Daneshfaraz et al., 2016; Toro et al., 2016) where the free surface is defined as the depth where there is a balance between water and air ($\alpha = 0.5$), a study similar to Lopes et al. (2018) was made where it was sought to define different values of water fraction (α) for the nonaerated and the aerated regions of the skimming flow, based on the depths observed in Sanagiotta & Marques (2008). The values that better fit the observed depths were $\alpha = 0.30$ for the nonaerated region of the flow and $\alpha = 0.10$ for the aerated region for spillways with channels with slope 1V:0.75H. However, as there are reports in the literature that the homogeneous model cannot correctly represent the air entrainment into the skimming flow, in future research, the results related to the definition of the free surface should be reevaluated with different multiphase models and meshes.

The model validation was also performed from velocity profiles along the chute, normal to the pseudobottom and starting at the outer edge of the steps. Velocity profiles were adjusted to a power law, with different exponents N: one for the nonaerated region and the other for the aerated region, both in agreement with the literature.

Mean pressures resulting from computational simulations and extreme pressures with different probability of occurrence obtained through a numerical-experimental approach were used to analyze uncertainties due to the relative position of the pressure gauges. To enable this analysis, the coefficients $N_{0.1\%}$ and $N_{99.9\%}$ and standard deviation values of the experimental data of Sanagiotta & Marques (2008) were calculated. With the use of these values, the mean pressures numerically obtained were used to estimate the extreme pressures ($P_{0.1\%}$ and $P_{99.9\%}$), which served as the criteria for the analysis of the effects in the experimental data of pressure due to the uncertainties in the position of piezometers and transducers.

From an analysis of the numerical results together with experimental data, it was determined that it is important that piezometers and transducers are located in the region of $0.81 < x/l < 0.98$ in horizontal faces and in the region of $0.93 < y/h < 0.98$ in vertical faces of steps. These results are initially valid for experimental studies in spillways with a slope of 1.0V:0.75H and a step height of 6 cm. If the criteria are respected, uncertainties due to the position of the instruments will not result in significant differences in the values of extreme pressures $P_{0.1\%}$ and $P_{99.9\%}$, even in full-scale prototype conditions.

ACKNOWLEDGEMENTS

This research was made possible through funding from R&D titled *Análise da Macroturbulência em Vertedouros em Degraus com Aeração Forçada (Pré-Aeração)* signed between DTEH.E/GST.E/FURNAS and FAURGS/IPH/UFRGS. This work has been partially supported by the Brazilian agency CAPES. The authors would like to acknowledge the anonymous reviewers for the constructive comments that benefitted the manuscript.

REFERENCES

- Albadawi, A., Donoghue, D. B., Robinson, A. J., Murray, D. B., & Delauré, Y. M. C. (2013). Influence of surface tension implementation in Volume of Fluid and coupled Volume of Fluid with Level Set methods for bubble growth and detachment. *International Journal of Multiphase Flow*, 53, 11-28. <http://dx.doi.org/10.1016/j.ijmultiphaseflow.2013.01.005>.
- Amador, A., Sánchez-Juny, M., & Dolz, J. (2009). Developing flow region and pressure fluctuations on steeply sloping stepped spillways. *Journal of Hydraulic Engineering*, 135(12), 1092-1100. [http://dx.doi.org/10.1061/\(ASCE\)HY.1943-7900.0000118](http://dx.doi.org/10.1061/(ASCE)HY.1943-7900.0000118).
- Ansys Inc. (2013). *Ansys CFX-solver theory guide, release 15.0*. Tokyo: Ansys, Inc.
- Arantes, E. J. (2007). *Caracterização do escoamento sobre vertedouros em degraus via CFD* (Tese de doutorado). Universidade de São Paulo, São Carlos.
- Arantes, E. J., Porto, R. M., Gulliver, J. S., Lima, A. C. M., & Schulz, H. E. (2010). Lower nappe aeration in smooth channels: experimental data and numerical simulation. *Anais da Academia Brasileira de Ciências*, 82(2), 521-537. <http://dx.doi.org/10.1590/S0001-37652010000200027>.
- Araújo Filho, M. F., & Ota, J. F. (2016). Modelagem computacional tridimensional de um vertedouro de baixa queda. *Revista Brasileira de Recursos Hídricos*, 21(2), 360-376. <http://dx.doi.org/10.21168/rbrh.v21n2.p360-376>.
- Aydin, M. C., & Ozturk, M. (2009). Verification and validation of a computational fluid dynamics (CFD) model for air entrainment at spillway aerators. *Canadian Journal of Civil Engineering*, 36(5), 826-836. <http://dx.doi.org/10.1139/L09-017>.
- Aydin, M. C., & Ozturk, M. (2010). Reply to discussion by Chanson and Lubin on "Verification and validation of a computational fluid dynamics (CFD) model for air entrainment at spillway aerators". *Canadian Journal of Civil Engineering*, 37(1), 139-142. <http://dx.doi.org/10.1139/L09-134>.
- Bai, Z. L., Peng, Y., & Zhang, J. M. (2017). Three-dimensional turbulence simulation of flow in a V-shaped stepped spillway. *Journal of Hydraulic Engineering*, 143(9), 06017011. [http://dx.doi.org/10.1061/\(ASCE\)HY.1943-7900.0001328](http://dx.doi.org/10.1061/(ASCE)HY.1943-7900.0001328).
- Bai, Z. L., & Zhang, J. (2017). Comparison of different turbulence models for numerical simulation of pressure distribution in V-shaped stepped spillway. *Mathematical Problems in Engineering*, 2017(3), 1-9. <http://dx.doi.org/10.1155/2017/3537026>.
- Bayon, A., Toro, J. P., Bombardelli, F. A., Matos, J., & López-Jiménez, P. A. (2018). Influence of VOF technique, turbulence model and discretization scheme on the numerical simulation of the non-aerated, skimming flow in stepped spillways. *Journal of Hydro-environment Research*, 19, 137-149. <http://dx.doi.org/10.1016/j.jher.2017.10.002>.
- Bindo, M., Gautier, J., & Lacroix, F. (1993). The stepped spillway of M'Bali dam. *International Water Power & Dam Construction*, 45(1), 35-36.
- Boes, R. M., & Hager, W. H. (2003). Two-phase flow characteristics of stepped spillways. *Journal of Hydraulic Engineering*, 129(9), 661-670. [http://dx.doi.org/10.1061/\(ASCE\)0733-9429\(2003\)129:9\(661\)](http://dx.doi.org/10.1061/(ASCE)0733-9429(2003)129:9(661)).
- Bombardelli, F. A., Meireles, I., & Matos, J. (2011). Laboratory measurements and multi-block numerical simulations of the mean flow and turbulence in the non-aerated skimming flow region of steep stepped spillways. *Environmental Fluid Mechanics*, 11(3), 263-288. <http://dx.doi.org/10.1007/s10652-010-9188-6>.
- Bung, D. B. (2011). Developing flow in skimming flow regime on embankment stepped spillways. *Journal of Hydraulic Research*, 49(5), 639-648. <http://dx.doi.org/10.1080/00221686.2011.584372>.
- Bung, D. B. (2013). Non-intrusive detection of air-water surface roughness in self-aerated chute flows. *Journal of Hydraulic Research*, 51(3), 322-329. <http://dx.doi.org/10.1080/00221686.2013.777373>.
- Celik, I. B., Ghia, U., Roache, P. J., Freitas, C. J., Coleman, H., Raad, P. E., Celik, I., Freitas, C., Coleman, H. P., & Raad, P. (2008). Procedure for estimation and reporting of uncertainty due to discretization in CFD applications. *Journal of Fluids Engineering*, 130(7), 078001-078004. <http://dx.doi.org/10.1115/1.2960953>.
- Çengel, Y. A., & Cimbala, J. M. (2006). *Fluid mechanics: fundamentals and applications* (1st ed.). New York: McGraw-Hill.
- Chanson, H. (1993). Stepped spillway flows and air entrainment. *Canadian Journal of Civil Engineering*, 20(3), 422-435. <http://dx.doi.org/10.1139/l93-057>.

- Chanson, H. (1994). *Hydraulic design of stepped cascade, channels, weirs and spillways*. Oxford: Elsevier Science.
- Chen, Q., Dai, G., & Liu, H. (2002). Volume of fluid model for turbulence numerical simulation of stepped spillway overflow. *Journal of Hydraulic Engineering*, 128(7), 683-688. [http://dx.doi.org/10.1061/\(ASCE\)0733-9429\(2002\)128:7\(683\)](http://dx.doi.org/10.1061/(ASCE)0733-9429(2002)128:7(683)).
- Conterato, E. (2011). *Escoamento sobre vertedouro em degraus com declividade 1V:0,75H: caracterização das pressões e condições de aeração* (Trabalho de conclusão de graduação). Universidade Federal do Rio Grande do Sul, Porto Alegre.
- Conterato, E. (2014). *Determinação de critérios de dimensionamento de soleira terminal em bacia de dissipação a jusante de vertedouro em degraus* (Dissertação de mestrado). Universidade Federal do Rio Grande do Sul, Porto Alegre.
- Conterato, E., Marques, M. G., & Alves, A. A. M. (2015). Proposta de uniformização das equações de previsão das características do escoamento sobre a calha de um vertedouro em degraus. *Revista Brasileira de Recursos Hídricos*, 20(1), 131-137. <http://dx.doi.org/10.21168/rbrh.v20n1.p131-137>.
- Dai Prá, M., Suzuki, L. E. A. S., Alves, A. A. M., & Marques, M. G. (2012). Um estudo sobre vertedouros em degraus de declividade 1V:1H. *Revista Recursos Hídricos*, 33(1), 17-28. <http://dx.doi.org/10.5894/rh33n1-2>.
- Daneshfaraz, R., Joudi, A. R., Ghahramanzadeh, A., & Ghaderi, A. (2016). Investigation of flow pressure distribution over a stepped spillway. *Advances and Applications in Fluid Mechanics*, 19(4), 805-822. <http://dx.doi.org/10.17654/FM019040811>.
- Dettmer, P. H. C., Ota, J. J., Fabiani, A. L. T., Araujo, A. L., & Franco, H. C. B. (2013). Simulação numérica da capacidade de descarga de um vertedouro de baixa queda afogado por jusante. In *Anais do XX Simpósio Brasileiro de Recursos Hídricos*. Porto Alegre: ABRH.
- Felder, S., & Chanson, H. (2011). Energy dissipation down a stepped spillway with nonuniform step heights. *Journal of Hydraulic Engineering*, 137(11), 1543-1548. [http://dx.doi.org/10.1061/\(ASCE\)HY.1943-7900.0000455](http://dx.doi.org/10.1061/(ASCE)HY.1943-7900.0000455).
- Ferziger, J. H., & Peric, M. (2002). *Computational methods for fluid dynamics* (3rd ed.). Berlin: Springer. <http://dx.doi.org/10.1007/978-3-642-56026-2>.
- Frizell, K. W., & Frizell, K. H. (2015). *Guidelines for hydraulic design of stepped spillways* (Hydraulic Laboratory Report, No. HL-2015-06). Denver: Bureau of Reclamation.
- Gabl, R., & Righetti, M. (2018). Design criteria for a type of asymmetric orifice in a surge tank using CFD. *Engineering Applications of Computational Fluid Mechanics*, 12(1), 397-410. <http://dx.doi.org/10.1080/19942060.2018.1443837>.
- Gomes, J. F. (2006). *Campo de pressões: condições de incipiência à cavitação em vertedouros em degraus com declividade 1V:0,75H* (Tese de doutorado). Universidade Federal do Rio Grande do Sul, Porto Alegre.
- Hirt, C. W., & Nichols, B. D. (1981). Volume of Fluid (VOF) methods for the dynamics of free boundaries. *Journal of Computational Physics*, 39(1), 201-225. [http://dx.doi.org/10.1016/0021-9991\(81\)90145-5](http://dx.doi.org/10.1016/0021-9991(81)90145-5).
- Jones, W. P., & Launder, B. E. (1972). The prediction of laminarization with a two-equation model of turbulence. *International Journal of Heat and Mass Transfer*, 15(2), 301-314. [http://dx.doi.org/10.1016/0017-9310\(72\)90076-2](http://dx.doi.org/10.1016/0017-9310(72)90076-2).
- Kositgittiwong, D., Chinnarasri, C., & Julien, P. Y. (2013). Numerical simulation of flow velocity profiles along a stepped spillway. *Proceedings of the Institution of Mechanical Engineers. Part E, Journal of Process Mechanical Engineering*, 227(4), 327-335. <http://dx.doi.org/10.1177/0954408912472172>.
- Launder, B. E., & Spalding, D. B. (1974). The numerical computation of turbulent flows. *Computer Methods in Applied Mechanics and Engineering*, 3(2), 269-289. [http://dx.doi.org/10.1016/0045-7825\(74\)90029-2](http://dx.doi.org/10.1016/0045-7825(74)90029-2).
- Li, D., Yang, Q., Ma, X., & Dai, G. (2018a). Case study on application of the step with non-uniform heights at the bottom using a numerical and experimental model. *Water*, 10(12), 1762. <http://dx.doi.org/10.3390/w10121762>.
- Li, S., Zhang, J., & Xu, W. (2018b). Numerical investigation of air-water flow properties over steep flat and pooled stepped spillways. *Journal of Hydraulic Research*, 56(1), 1-14. <http://dx.doi.org/10.1080/00221686.2017.1286393>.
- Lobosco, R. J., & Schulz, H. E. (2010). Análise computacional do escoamento em estruturas de vertedouros em degraus. *Mecânica Computacional*, XXIX, 3593-3600.
- Lopardo, R. A., Fattor, C., & Lopardo, M. (2004). Instantaneous pressure field on a submerged jump stilling basin. In F. Yazdandoost & J. Attari (Eds.), *Proceedings of the International Conference on Hydraulics of Dams and River Structures*. Tehran: A. A. Balkema Publishers. <http://dx.doi.org/10.1201/b16994-19>.
- Lopes, P., Leandro, J., & Carvalho, R. F. (2018). Numerical procedure for free-surface detection using a Volume-of-Fluid model. *Journal of Hydro-Environment Research*, 21, 43-51. <http://dx.doi.org/10.1016/j.jher.2018.07.002>.
- Ma, L., Ashworth, P. J., Best, J. L., Elliott, L., Ingham, D. B., & Whitcombe, L. J. (2002). Computational fluid dynamics and the physical modelling of an upland urban river. *Geomorphology*, 44(3-4), 375-391. [http://dx.doi.org/10.1016/S0169-555X\(01\)00184-2](http://dx.doi.org/10.1016/S0169-555X(01)00184-2).
- Meireles, I. C., Bombardelli, F. A., & Matos, J. (2014). Air entrainment onset in skimming flows on steep stepped spillways: an analysis. *Journal of Hydraulic Research*, 52(3), 375-385. <http://dx.doi.org/10.1080/00221686.2013.878401>.

- Meireles, I., Renna, F., Matos, J., & Bombardelli, F. (2012). Skimming, nonaerated flow on stepped spillways over roller compacted concrete dams. *Journal of Hydraulic Engineering*, 138(10), 870-877. [http://dx.doi.org/10.1061/\(ASCE\)HY.1943-7900.0000591](http://dx.doi.org/10.1061/(ASCE)HY.1943-7900.0000591).
- Novakoski, C. K., Conterato, E., Marques, M., Teixeira, E. D., Lima, G. A., & Mees, A. (2017a). Macro-turbulent characteristics of pressures in hydraulic jump formed downstream of a stepped spillway. *Revista Brasileira de Recursos Hídricos*, 22(e22), 8.
- Novakoski, C. K., Hampe, R. F., Conterato, E., Marques, M. G., & Teixeira, E. D. (2017b). Longitudinal distribution of extreme pressures in a hydraulic jump downstream of a stepped spillway. *Revista Brasileira de Recursos Hídricos*, 22(e42), 8. <http://dx.doi.org/10.1590/2318-0331.0117160035>.
- Osmar, F. M., Canellas, A. V. B., Priebe, P. S., Saraiva, L. S., Teixeira, E. D., & Marques, M. G. (2018). Analysis of the longitudinal distribution of pressures near the ends of the vertical and horizontal faces in stepped spillway of slope 1V:0.75H. *Revista Brasileira de Recursos Hídricos*, 23(e4), 11. <http://dx.doi.org/10.1590/2318-0331.0318170057>.
- Pfister, M., & Hager, W. H. (2010a). Chute aerators. I: air transport characteristics. *Journal of Hydraulic Engineering*, 136(6), 352-359. [http://dx.doi.org/10.1061/\(ASCE\)HY.1943-7900.0000189](http://dx.doi.org/10.1061/(ASCE)HY.1943-7900.0000189).
- Pfister, M., & Hager, W. H. (2010b). Chute aerators. II: hydraulic design. *Journal of Hydraulic Engineering*, 136(6), 360-367. [http://dx.doi.org/10.1061/\(ASCE\)HY.1943-7900.0000201](http://dx.doi.org/10.1061/(ASCE)HY.1943-7900.0000201).
- Pfister, M., & Hager, W. H. (2014). History and significance of the morton number in hydraulic engineering. *Journal of Hydraulic Engineering*, 140(5), 02514001. [http://dx.doi.org/10.1061/\(ASCE\)HY.1943-7900.0000870](http://dx.doi.org/10.1061/(ASCE)HY.1943-7900.0000870).
- Qian, Z., Hu, X. Q., Huai, W. X., & Amador, A. (2009). Numerical simulation and analysis of water flow over stepped spillways. *Science in China Series E: Technological Sciences*, 52(7), 1958-1965. <http://dx.doi.org/10.1007/s11431-009-0127-z>.
- Roache, P. J. (1994). Perspective: a method for uniform reporting of grid refinement studies. *Journal of Fluids Engineering*, 116(3), 405-413. <http://dx.doi.org/10.1115/1.2910291>.
- Sanagioto, D. G. (2003). *Características do escoamento sobre vertedouros em degraus de declividade 1V:0,75H* (Dissertação de mestrado). Universidade Federal do Rio Grande do Sul, Porto Alegre.
- Sanagioto, D. G., & Marques, M. G. (2008). Características do escoamento em vertedouros em degraus de declividade 1V:0,75H. *Revista Brasileira de Recursos Hídricos*, 13(4), 17-31. <http://dx.doi.org/10.21168/rbrh.v13n4.p17-31>.
- Sanagioto, D., Rossi, J., & Bravo, J. (2019a). Applications of computational fluid dynamics in the design and rehabilitation of nonstandard vertical slot fishways. *Water*, 11(2), 199. <http://dx.doi.org/10.3390/w11020199>.
- Sanagioto, D. G., Rossi, J. B., Lauffer, L. L., & Bravo, J. M. (2019b). Three-dimensional numerical simulation of flow in vertical slot fishways: validation of the model and characterization of the flow. *Revista Brasileira de Recursos Hídricos*, 24(20), 14. <http://dx.doi.org/10.1590/2318-0331.241920180174>.
- Sánchez-Juny, M., Bladé, E., & Dolz, J. (2007). Pressures on a stepped spillway. *Journal of Hydraulic Research*, 45(4), 505-511. <http://dx.doi.org/10.1080/00221686.2007.9521785>.
- Simões, A. L. A. (2012). *Escoamentos turbulentos em canais com o fundo em degraus: resultados experimentais, soluções numéricas e proposições teóricas* (Tese de doutorado). Universidade de São Paulo, São Carlos.
- Simões, A. L. A., Schulz, H. E., & Porto, R. M. (2010). Stepped and smooth spillways: resistance effects on stilling basin lengths. *Journal of Hydraulic Research*, 48(3), 329-337. <http://dx.doi.org/10.1080/00221686.2010.481853>.
- Simões, A. L. A., Schulz, H. E., Porto, R. M., & Gulliver, J. S. (2013). Free-surface profiles and turbulence characteristics in skimming flows along stepped chutes. *Journal of Water Resource and Hydraulic Engineering*, 2(1), 1-12.
- Stenmark, E. (2013). *On multiphase flow models in ANSYS CFD software* (Master thesis). Chalmers University of Technology, Göteborg, Sweden.
- Tabari, M. M. R., & Tavakoli, S. (2016). Effects of stepped spillway geometry on flow pattern and energy dissipation. *Arabian Journal for Science and Engineering*, 41(4), 1215-1224. <http://dx.doi.org/10.1007/s13369-015-1874-8>.
- Tabbara, M., Chatila, J., & Awwad, R. (2005). Computational simulation of flow over stepped spillways. *Computers & Structures*, 83(27), 2215-2224. <http://dx.doi.org/10.1016/j.compstruc.2005.04.005>.
- Teixeira, E. D. (2008). *Efeito de escala na previsão dos valores extremos de pressão junto ao fundo em bacias de dissipação por ressalto hidráulico* (Tese de doutorado). Universidade Federal do Rio Grande do Sul, Porto Alegre.
- Teng, P., & Yang, J. (2016). CFD modeling of two-phase flow of a spillway chute aerator of large width. *Journal of Applied Water Engineering and Research*, 4(2), 163-177. <http://dx.doi.org/10.1080/023249676.2015.1124030>.
- Toro, J. P., Bombardelli, F. A., Paik, J., Meireles, I., & Amador, A. (2016). Characterization of turbulence statistics on the non-aerated skimming flow over stepped spillways: a numerical study. *Environmental Fluid Mechanics*, 16(6), 1195-1221. <http://dx.doi.org/10.1007/s10652-016-9472-1>.
- Tozzi, M. J. (1992). *Caracterização/comportamento de escoamentos em vertedouros com paramento em degraus* (Tese de doutorado). Universidade de São Paulo, São Paulo.

- Van Alwon, J., Borman, D., Matos, J., Kapur, N., & Sleigh, A. (2019). Prediction of air entrainment in skimming flow over stepped spillways using numerical methods. In *Proceedings of the 38th LAHR World Congress 2019*. Panama City, Panama: International Association for Hydro-Environment Engineering and Research.
- Van Alwon, J., Borman, D., Sleigh, A., & Kapur, N. (2017). Experimental and numerical modelling of aerated flows over stepped spillways. In *Proceedings of the 37th LAHR World Congress 2017*. Kuala Lumpur, Malaysia: International Association for Hydro-Environment Engineering and Research.
- Yang, J., Teng, P., & Zhang, H. (2019). Experiments and CFD modeling of high-velocity two-phase flows in a large chute aerator facility. *Engineering Applications of Computational Fluid Mechanics*, 13(1), 48-66. <http://dx.doi.org/10.1080/19942060.2018.1552201>.
- Zhan, J., Zhang, J., & Gong, Y. (2016). Numerical investigation of air-entrainment in skimming flow over stepped spillways. *Theoretical and Applied Mechanics Letters*, 6(3), 139-142. <http://dx.doi.org/10.1016/j.taml.2016.03.003>.
- Zhang, G., & Chanson, H. (2016a). Hydraulics of the developing flow region of stepped spillways. ii: pressure and velocity fields. *Journal of Hydraulic Engineering*, 142(7), 04016015. [http://dx.doi.org/10.1061/\(ASCE\)HY.1943-7900.0001138](http://dx.doi.org/10.1061/(ASCE)HY.1943-7900.0001138).
- Zhang, G., & Chanson, H. (2016b). Hydraulics of the developing flow region of stepped spillways. I: physical modeling and boundary layer development. *Journal of Hydraulic Engineering*, 142(7), 04016015. [http://dx.doi.org/10.1061/\(ASCE\)HY.1943-7900.0001138](http://dx.doi.org/10.1061/(ASCE)HY.1943-7900.0001138).
- Zhang, J., Chen, J., & Wang, Y. (2012). Experimental study on time-averaged pressures in stepped spillway. *Journal of Hydraulic Research*, 50(2), 236-240. <http://dx.doi.org/10.1080/00221686.2012.666879>.

Authors contributions

Lucas Camargo da Silva Tassinari: Conceptualization, methodology, simulations, validation, formal analysis and writing of the paper.

Daniela Guzzon Sanagiotto: Conceptualization, methodology, formal analysis and writing of the paper.

Marcelo Giulian Marques: Conceptualization, project administration and review of the text.

Luísa Lüdtke Lauffer: Simulations, validation and formal analysis.

Edgar Fernando Trierweiler Neto: Formal analysis and review of the text.